missing oocyte encodes a highly conserved nuclear protein required for the maintenance of the meiotic cycle and oocyte identity in *Drosophila*

Takako Iida and Mary A. Lilly*

Cell Biology and Metabolism Branch, National Institute of Child Health and Human Development, National Institutes of Health, Bethesda, MD 20892, USA
*Author for correspondence (e-mail: mlilly@helix.nih.gov)

Accepted 17 November 2003

Development 131, 1029-1039
Published by The Company of Biologists 2004
doi:10.1242/dev.01001

Summary

In *Drosophila*, a single oocyte develops within a 16-cell germline cyst. Although all 16 cells initiate meiosis and undergo premeiotic S phase, only the oocyte retains its meiotic chromosome configuration and remains in the meiotic cycle. The other 15 cells in the cyst enter the endocycle and develop as polyploid nurse cells. A long-standing goal in the field has been to identify factors that are concentrated or activated in the oocyte, that promote meiotic progression and/or the establishment of the oocyte identity. We present the characterization of the *missing oocyte* gene, an excellent candidate for a gene directly involved in the differentiation of the oocyte nucleus. The *missing oocyte* gene encodes a highly conserved protein that preferentially accumulates in pro-oocyte nuclei in early prophase of meiosis I. In *missing oocyte* mutants, the oocyte enters the endocycle and develops as a polyploid nurse cell. Genetic interaction studies indicate that *missing oocyte* influences meiotic progression prior to pachytene and may interact with pathways that control DNA metabolism. Our data strongly suggest that the product of the *missing oocyte* gene acts in the oocyte nucleus to facilitate the execution of the unique cell cycle and developmental programs that produce the mature haploid gamete.

Supplemental data available online

Key words: Meiosis, Oogenesis, *Drosophila*, Synaptonemal complex, Oocyte differentiation

Introduction

During the development of a multicellular animal, cell growth and proliferation must be spatially and temporally coordinated with differentiation. Nowhere is this more important than during gametogenesis where meiosis, which involves a fundamental reorganization of the cell cycle, must be precisely coordinated with the developmental program to make an egg or a sperm. *Drosophila* oogenesis provides a genetically tractable system to examine how the early events of meiosis are coordinated with the ongoing differentiation of the oocyte.

Drosophila oogenesis starts when a cystoblast, the asymmetric daughter of the germline stem cell, undergoes four divisions with incomplete cytokinesis to produce a 16-cell interconnected cyst (Fig. 1A). Individual cells in the cyst, referred to as cystocytes, are connected by actin-rich intercellular bridges called ring canals (Robinson and Cooley, 1996). All 16 cystocytes complete a long premeiotic S phase. Subsequently, the two cystocytes with four-ring canals, the pro-oocytes, develop long synaptonemal complexes (SC) consistent with pachytene of meiotic prophase I (Mahowald and Kambysellis, 1980). Several other cells show similar but reduced SC structures; however, only the true oocyte maintains its meiotic state and further condenses its chromatin. The other 15 cystocytes lose their meiotic characteristics, enter the endocycle and develop as polyploid nurse cells.

Oocyte differentiation, as well as the maintenance of the meiotic cycle, are dependent on the microtubule-based directional transport of specific mRNAs and proteins from the nurse cells to the oocyte (Fig. 1B) (Cooley and Theurkauf, 1994). When directional transport to the oocyte is disrupted either chemically by disassembling microtubules, or genetically as occurs in the *Bicaudal-D* (*Bic-D*) and *Lis-1* mutants, egg chambers fail to localize oocyte specific markers and develop with 16-polyploid nurse cells and no oocyte (Koch and Spitzer, 1985; Suter and Steward, 1991; Theurkauf et al., 1993; Mach and Lehmann, 1997; Liu et al., 1999; Swan et al., 1999). In *egl* mutants, in which directional transport to the oocyte is also disrupted, all 16 cystocytes initially behave like pro-oocytes and proceed to early pachytene before reverting to the nurse cell fate and entering the endocycle (Carpenter, 1994; Mach and Lehmann, 1997). This observation supports the model that the cell-cycle and developmental signals required for oocyte development are initially present in all cystocytes but are concentrated in the single oocyte during early meiotic prophase I (Suter and Steward, 1991; Carpenter, 1994; Mach and Lehmann, 1997).

Several lines of evidence indicate that oocyte differentiation is contingent on the execution of the proper cell-cycle program of the germline cyst. As is observed in all

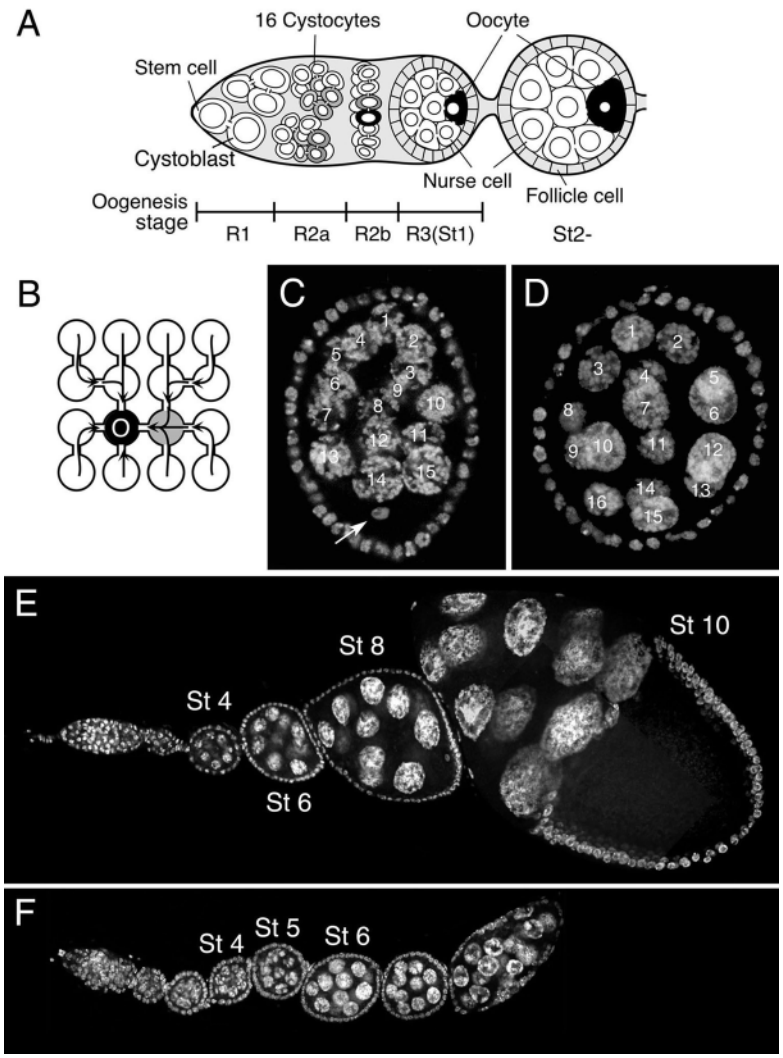

Fig. 1. *mio* is required for oocyte development. (A) The cell types and stages of *Drosophila* oogenesis. In region 1 of the germarium (R1), a germline stem cell divides to give rise to a cyst of 16 interconnected cystocytes. In region 2a (R2a), the two pro-oocytes (dark grey), as well as the two adjacent cells with three ring canals (light grey), construct SC. The meiotic gradient is restricted to the single oocyte by region 3 (stage 1). In region 3, the nurse cells enter the endocycle. (B) Microtubule-based directional transport to the oocyte (black). (C) A wild-type stage 5 egg chamber. Note that the oocyte DNA has condensed into a compact karyosome (arrow). (D) A *mio*^{2} egg chamber that contains 16-polyploid nurse cells. (E,F) Ovarioles from wild-type (E) and *mio*^{2} homozygous female (F). Ovarioles were stained with Hoechst to visualize nuclei. O, oocyte.

animal oocytes, in *Drosophila* the oocyte arrests in prophase of meiosis I for the growth phase of oogenesis. During this developmentally programmed arrest, the p27-like cyclin-dependent kinase inhibitor Dacapo (Dap) specifically accumulates in the oocyte nucleus (de Nooij et al., 2000; Hong et al., 2003). The characterization of *dap* mutants suggests that Dap inhibits inappropriate DNA replication in oocyte and thus helps maintain the prophase I meiotic arrest (Hong et al., 2003). In the absence of Dap, the oocyte enters the endocycle and develops as a nurse cell. Thus, inappropriate entry into the endocycle disrupts oocyte differentiation and can serve as the primary cause of the loss of the oocyte fate. The characterization of two genes required to repair double-strand breaks (DSBs) during meiosis demonstrate that meiotic progression and oocyte differentiation are tightly coupled. The formation of the both the anteroposterior and dorsoventral axis of the oocyte is dependent on activity of Gurken (Grk), the TGFα-like ligand for EGF receptor (Egfr) (reviewed by Van Buskirk and Schüpbach, 1999). In *okra* (*okr*) and *spindle-B* (*spnB*) mutants the translation of the *grk* transcript is inhibited, resulting in pattern defects similar to those produced by mutants in the *grk-Egfr* signaling pathway (Gonzalez-Reyes et al., 1997; Ghabrial et al., 1998). Surprisingly, *okr* and *spnB* encode the *Drosophila* homologs of the yeast DSB repair proteins, RAD54 and DMC1. These data indicate that the pathways that control DSB repair specifically influence the *grk-Egfr* signaling pathway during oogenesis (Ghabrial et al., 1998).

Why does the oocyte nucleus progress through meiosis while adjacent cystocytes abandon the meiotic cycle in preparation for their development as nurse cells? Although this question is fundamental to a comprehensive understanding of oocyte development, little is known about the pathways that directly promote the differentiation of the oocyte nucleus. We describe the identification and characterization of a novel gene, *missing oocyte* (*mio*) that is required for the maintenance of the meiotic cycle during oogenesis. We cloned the *mio* gene and determined that the Mio protein localizes to the oocyte nucleus at the onset of prophase of meiosis I. In *mio* mutants, oocyte differentiation and meiotic progression are retarded. Ultimately, *mio* oocytes exit the meiotic cycle, enter the endocycle and develop as nurse cells. Surprisingly, the *mio* phenotype is suppressed by inhibiting the formation of the double-stranded breaks that initiate meiotic recombination. Our data strongly suggest that *mio* mutants define a novel pathway that influences both the nuclear events of meiotic progression and oocyte differentiation.

Materials and methods

Drosophila strains and genetics

The *mio*^{1} allele was isolated from ~2000 ethylmethane sulfonate (EMS)-mutagenized chromosomes in a screen for mutations that disrupt cell-cycle regulation in the ovary (K. O'Donnell and M. A. Lilly, data not shown). The *mio*^{2} allele was identified as a background mutation on a chromosome that contained the *stand still*^{3} allele (*stil*^{3}). *stil*^{3} was isolated in an EMS mutagenesis (Mulligan et al., 1996). *egl*^{1} (*egl*^{WU}) and *Df(2R)vg135* were obtained from Umea Drosophila Stock Center (Sweden) (Schüpbach and Wieschaus, 1991). *egl*^{2}(*egl*^{RC12}), *stil*^{1} and *stil*^{2} were a gift from T. Schüpbach (Schüpbach and Wieschaus, 1991). *Df(2L)yan*^{J2} was a gift from Z. C. Lai (Lai et al., 1997). *mei-41* null mutant, *mei-41*^{29D}, was a gift from T. T. Su (Laurençon et al., 2003). All additional stocks were obtained from the Bloomington Stock Center.

Molecular characterization of the *mio* gene

We mapped the *mio* locus between the proximal breakpoints of *Df(2L)dp*^{79b} and *Df(2L)yan*^{J2}. To physically map the extent of this chromosomal region, we determined the molecular breakpoints of the deficiencies by quantitative Southern blot analysis. This analysis indicated *mio* mapped to a 50 kb genomic region, between 22C3 and 22D2, which contained 11 predicted open reading frames (ORFs) (FlyBase). From these 11 ORFs, all predicted exons were amplified from genomic DNA samples of *mio*^{1} and *mio*^{2} homozygous flies, sequenced and then compared with the sequence from the Berkeley Drosophila Genome Project (BDGP). To confirm that the single nucleotide changes found in *CG7074* were not due to random polymorphisms, we sequenced the appropriate parental chromosomes, *y*^{1}, *w*^{1118}, *P{y*$^{+t7.7}$ *ry*$^{+t7.2}$*=Car20y}25F P{ry*$^{+t7.2}$*=neoFRT}40A* and Canton S.

The *CG7074*-coding region was identified by 5′ and 3′ RACE of mio cDNA using the primers, 5′-GCCGCCGACGATAGGATGTT-GCAGGC-3′ and 5′-ACTCAGCAGCAGCCCACGAGCAGC-3′, respectively, and the SMART RACE cDNA Amplification Kit (Clontech). Full-length *mio* cDNA was amplified by RT-PCR, cloned into pCR II-TOPO and sequenced. The *mio* cDNA sequence is available as the *mio* gene in AE003584 GenBank sequence.

UASp:mio rescue

The full-length *mio* cDNA was cloned into the pUASp vector (Rørth, 1998) from the pCR II-TOPO vector. Transgenic lines were generated in a *w*^{1118} background using standard techniques (Spradling, 1986). Three independent insertions were obtained, all of which mapped to the second chromosome. Therefore, we crossed the *UASp-mio* P-element onto the *mio*^{2} chromosome using meiotic recombination. We expressed *UASp-mio* in the *mio*^{2} mutant background using the nanos-Gal4:VP16 driver (Van Doren et al., 1998).

Production of anti-Mio antibodies

Nucleotides 1865 to 2473 of the *mio* cDNA (LD45056) were amplified using primers that added a *Bam*HI site to the 5′ end and an *Xho*I site to the 3′ end, and cloned into pET21a (Novagen) to generate a His-tag fusion protein. The fusion protein contains amino acids 601-803 of the Mio protein tagged with a 6x His tag at the C terminus. The fusion proteins was expressed in *Escherichia coli* BL21 cells (Novagen) and purified on a nickel column before being used as antigen to produce rabbit polyclonal anti-Mio antibodies.

Immunostaining and imaging

Immunostaining of ovaries was performed as described previously (Grieder et al., 2000). The rabbit αMio antiserum was used at a concentration of 1:1000. Other antibodies were used at the following concentrations: rabbit αC(3)G (Hong et al., 2003) at 1:1000, mouse αOrb 6H4 (Lantz et al., 1994) at 1:50 (purified IgG, Developmental Studies Hybridoma Bank, University of Iowa), mouse αBic-D (Suter and Steward, 1991) at 1:5 dilutions. Secondary antibodies conjugated to Alexa 594 or Alexa 488 (Molecular Probes) were used at 1:800 dilution. Double labeling of rabbit antibodies, αMio and αC(3)G was performed using αC(3)G antibody that was directly labeled with Alexa 594 (Alexa Fluor 594 Protein Labeling Kit, Molecular Probes). Nuclei were visualized with 2 μg/ml Hoechst 33342 (Molecular Probes). Confocal images of stained ovaries were captured on a LSM 410 confocal microscope (Zeiss) with a 1.4 NA 63× oil immersion objective or a 1.4 NA 100× oil immersion objective. Image analysis was performed using LSM imaging software. Composite figures were prepared using Photoshop 5.5 (Adobe).

Western analysis

Ovaries were dissected in Grace's medium (Gibco) and homogenized in (50 mM Tris-HCl pH 7.5, 1 mM $MgCl_2$, 1 mM PMSF). After centrifugation to pellet the debris, supernatants were diluted with an equal volume of 2×SDS loading buffer (Bio Rad), resolved by 7.5% SDS-polyacrylamide gels, and transferred to Hybond ECL nitrocellulose membrane (Amersham). αMio serum was used at 1:3000. As a loading control, blots were probed with anti-αTubulin antibody at 1:9000 (DM 1A, Sigma). For detection, blots were incubated with Horseradish Peroxidase-conjugated antibody (Amersham) at a 1:6000 dilution, and bands were visualized with a chemiluminescent detection kit (Amersham).

Results

mio egg chambers contain 16-polyploid nurse cells

We performed a genetic screen to isolate mutants that alter the cell cycle of the ovarian cyst. From this screen we identified *mio*, a mutant that produced a high percentage of egg chambers with 16-polyploid nurse cells. In 80%-90% (Table 1) of the egg chambers from *mio*^{1} mutant females, all 16 cystocytes enter the endocycle and develop as nurse cells (Fig. 1D). *mio* egg chambers rarely develop beyond stage 5 of oogenesis (Fig. 1F). Thus, *mio* ovarioles contain numerous developmentally arrested egg chambers of approximately the same size. During complementation analysis with known female sterile mutants, a second *mio* allele was fortuitously identified as a background mutation on the *stl*^{3} chromosome (see Materials and methods). Both *mio*^{1} and *mio*^{2} are homozygous viable and female sterile. The female sterility and 16 nurse cell phenotype is fully recessive in both alleles. Neither the penetrance nor the expressivity of the *mio* phenotype is increased when *mio*^{1} or *mio*^{2} are placed in trans to a deficiency, suggesting that both alleles are genetic nulls (Table 1). However, we note that the severity of the *mio*^{1}/Df ovarian phenotype is somewhat reduced relative to that observed in *mio*^{1} homozygotes, indicating that *mio*^{1} may be a weak antimorph.

Mio is required for the maintenance of the oocyte identity

There are at least two developmental times, which are not mutually exclusive, when *mio* may act to influence oocyte identity. First, *mio* may be required for the specification and early differentiation of the oocyte. Alternatively, *mio* may act later in oogenesis to maintain oocyte identity. Mutations that block either the specification of the oocyte, or the maintenance of oocyte identity, result in the same phenotype; the production of egg chambers with 16-polyploid nurse cells. One way to distinguish between these two mutant classes is to examine the localization of oocyte specific markers. Mutants with a block in oocyte specification and/or the establishment of cyst polarity such as *Bic-D*, *egl* and *Lis-1*, never localize oocyte specific markers (Suter and Steward, 1991; Lantz et al., 1992; Lantz et al., 1994; Ran et al., 1994; Swan et al., 1999; Huynh and St

Table 1. Phenotypes of *mio* mutant egg chambers

Maternal genotype	*n*	16-nurse cell (%)	Eight-nurse cell (%)	Other* (%)	Wild type (%)
mio^{1}/+	73	0	0	1.4	98.6
mio^{1}/*mio*^{1}	104	80.8	0	6.7	12.5
mio^{1}/*Df*	246	63.8	0	1.6	34.6
mio^{2}/*mio*^{2}	52	90.4	5.8	1.4	1.9
mio^{2}/*Df*	159	80.5	3.8	0	15.7
mio^{1}/*mio*^{2}	722	94.3	0.6	0	5.1

*Egg chambers that have more than 16 cells, or that have mislocalized oocyte.

Johnston, 2000). In contrast, mutants such as *stonewall*, *par-1* and *dap*, that disrupt the maintenance but not the specification of the oocyte identity, initially localize oocyte specific markers but this localization is lost when the oocyte inappropriately enters the endocycle (Clark and McKearin, 1996; Huynh et al., 2001; Vaccari and Ephrussi, 2002; Hong et al., 2003).

In order to determine if *mio* influences the specification of the oocyte identity, we examined the localization of Orb and Bic-D protein in *mio* mutant ovaries. In wild-type cysts, the Orb and Bic-D proteins first accumulate in the cytoplasm of the oocyte, as well as that of several adjacent cells, in region 2a of the germarium soon after the completion of premeiotic S phase (Fig. 2A) (Christerson and McKearin, 1994; Lantz et al., 1994). As cysts pass through region 2b Orb and Bic-D staining becomes restricted to a single centrally localized cell, which will ultimately become the oocyte. *mio* cysts clearly specify an oocyte, as indicated by the specific accumulation of Orb and Bic-D protein within a single cell (Fig. 2B, and data not shown).

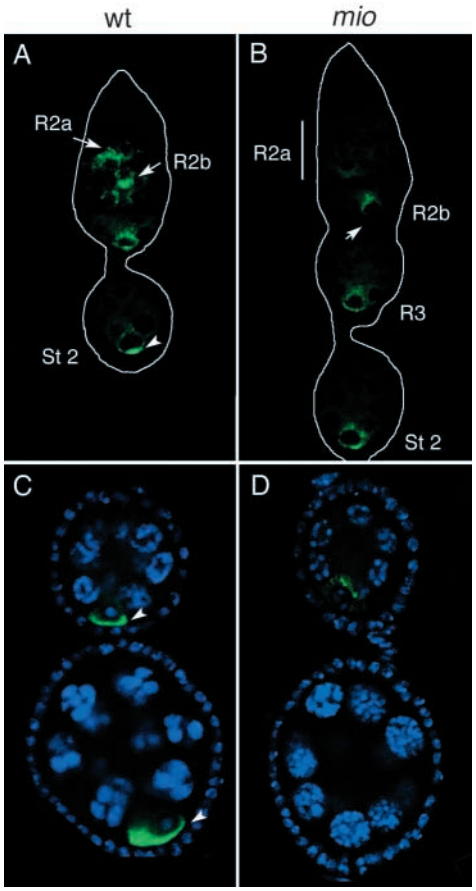

Fig. 2. αOrb staining in wild-type and *mio* ovaries. Wild-type (A,C) and *mio* mutant (B,D) germaria stained with αOrb (green) and Hoechst (blue). (A) In wild type, weak Orb accumulation is first observed in a single cell in region 2a (arrow), and becomes strong by region 2b. (B) In *mio* mutants, Orb accumulation in a single cell is not visible until late region 2b (arrow) or sometime until region 3. (C) In wild type, Orb continues to accumulate at the posterior cortex of the oocyte during post-germarial stages (arrowheads). (D) In *mio* mutant egg chambers, some Orb proteins do not move to the posterior in stage 2 (see B), remain detectable in the anterior of the oocyte, and gradually disappear when the oocyte enters the endocycle.

However, the preferential accumulation of Orb in the mutant pro-oocytes is markedly delayed and is often not visible until late region 2b or region 3 (Fig. 2B). Indeed, the overall levels of Orb appear to be lower in *mio* mutants (Fig. 2A,B).

Although *mio* mutants specify an oocyte, this fate is not maintained in the later stages of oogenesis. In wild-type ovaries, Bic-D and Orb continue to accumulate in post-germarial egg chambers following a shift in their localization from the anterior to the posterior of the oocyte in stage 2 (Fig. 2A,C) (Wharton and Struhl, 1989; Lantz et al., 1994). This translocation reflects a reorganization of the polarity of the microtubules within the oocyte (Theurkauf et al., 1992; Pare and Suter, 2000; Vaccari and Ephrussi, 2002). However, in *mio* mutants Orb and Bic-D frequently do not move to the posterior of the oocyte in stage 2 (Fig. 2B). In addition, the preferential accumulation of Orb and Bic-D is gradually lost when the oocyte becomes polyploid later in oogenesis and reverts to the nurse cell fate (Fig. 2D, and data not shown). Thus, in *mio* mutants the acquisition of the oocyte identity is delayed and the oocyte fate is not maintained in post-germarial egg chambers.

Null mutations in the cyclin-dependent kinase inhibitor *dap* have a similar effect on the maintenance of oocyte identity (Hong et al., 2003). In *dap* mutants, an oocyte is initially specified. However, once the oocyte enters the endocycle, the oocyte identity is gradually lost and egg chambers develop with 16 polyploid nurse cells. We wanted to examine if *mio* influences oocyte differentiation by regulating Dap expression. In the ~10% of the mio^2 egg chambers in which the oocyte does not enter the endocycle, Dap protein accumulates to high levels in the single oocyte as is observed in wild-type egg chambers. These data indicate that Dap can be expressed and properly localized to the oocyte nucleus in the absence of Mio. In the 90% of egg chambers in which the oocyte becomes polyploid, Dap does not accumulate to high levels in any one cell. Thus, as is observed with all oocyte-specific markers examined, the specific accumulation of Dap is lost, or is never properly established, in *mio* oocytes that enter the endocycle. We believe this reflects a general problem in the maintenance of oocyte identity and/or the differential transport system, as represented by the concomitant loss of Bic-D and Orb accumulations, rather than a direct role for Mio in the regulation of Dap expression. However, we cannot rule out the formal possibility that some aspects of the *mio* ovarian phenotype are due to the misregulation of Dap.

Meiotic progression is altered in *mio* mutants

To examine if Mio is required for early meiotic progression, we followed the distribution of the SC protein C(3)G. In wild-type cysts, the two pro-oocytes progress to pachytene in region 2a as determined by the completion of the SC along all bivalents (Mahowald and Kambysellis, 1980) (Fig. 3A). Cells adjacent to the pro-oocyte also build a less extensive network of SC. In *mio* mutants, an increased number of cells enter the meiotic cycle in region 2a as assayed by C(3)G staining (6.5±2.1, n=21 versus 3.9±.3, n=14 in wild type) with 76% of *mio* cysts having more than five cells in the meiotic cycle (Fig. 3B). Although too many cells enter meiosis, *mio* mutants retain the ability to restrict the meiotic cycle to a single cell. Thus, as is observed in wild type, by region 3 the majority of *mio* cysts contain a single C(3)G positive cell (Fig. 3B).

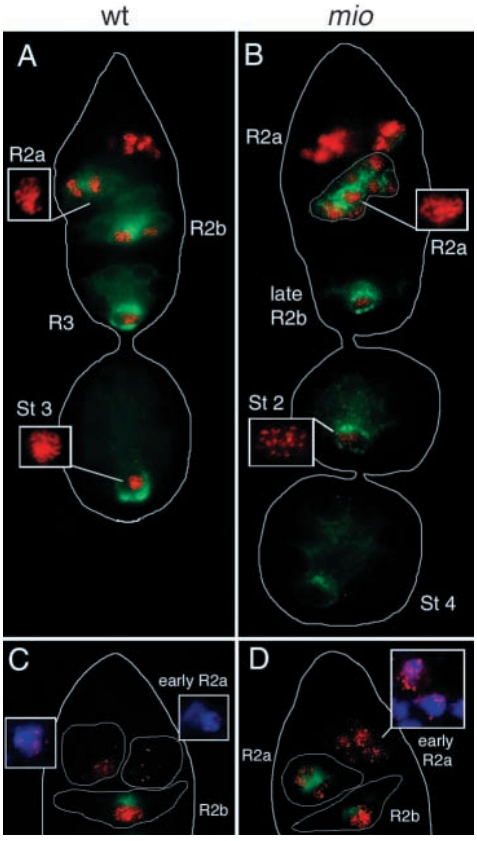

Fig. 3. *mio* affects meiotic progression. Wild-type (A) and *mio* mutant germaria (B) stained with αC(3)G (red) and αOrb (green). Magnified C(3)G staining of adjacent cysts are shown in small boxes. As is observed in wild type, in *mio* mutants fully developed SCs are formed in two to four cells in region-2a cyst. However, in *mio* cysts more than four cells enter the meiotic cycle and construct SC (see region-2a cyst traced with white line). (C,D) Anterior regions of wild type (C) and *mio* mutant germaria (D). Boxes indicate magnified regions of adjacent cysts stained with Hoechst (blue) and C(3)G (red). (C) Upper two cysts traced with white line are in early region 2a, determined by the absence of Orb expression. In wild type, early region-2a cysts sometimes show an early zygotene-like SC, with two to ten dots per nucleus observed in one or two cystocyte within a cyst. (D) In *mio* mutants, more extensive SCs are observed in early region 2a, which include numerous dots and short thread-like SCs that are often present in more than two cells per cyst.

mio mutant germaria contain cysts that have pro-oocytes with a pachytene-like SC configuration, indicating that Mio is not an absolute requirement for entry into the meiotic cycle or for progression to pachytene (Fig. 3B). However, Mio does affect the kinetics of SC formation. Relative to wild type, *mio* germaria contain approximately twice as many cysts in region 2a (21.7%, n=106 in wild type versus 50.7%, n=67 in *mio* mutants) in which the pro-oocytes appear to be in early or late zygotene and thus contain fragmented and/or partially formed SC. Specifically, *mio* mutants have a large number of 2a cysts that have the broken SC structure suggestive of late-zygotene or early-pachytene (Fig. 3C,D). The apparent increase in the proportion of cysts at this intermediate step in meiosis may represent either a delay in SC construction or the formation of aberrant SC. These data indicate that Mio influences meiotic progression and/or the establishment of meiotic chromosome structure during early prophase of meiosis I.

Mio is required for progression to pachytene in *egl* mutants

To explore the function of *mio* further during oogenesis, we made double-mutant combinations of *mio* and *egl*. In *egl* mutants, all 16-cyst cells enter the meiotic cycle and form SCs (Carpenter, 1994; Page and Hawley, 2001) (Fig. 4B). However, this meiotic state is not stably maintained and ultimately all 16 cystocytes exit the meiotic cycle and enter the endocycle. We generated females that were double mutant for mio^2 and one of two null alleles of *egl*, egl^1 or egl^2. Intriguingly, *mio, egl* females have an ovarian phenotype significantly stronger than either single mutant. *mio, egl* double mutants do not form even the thin SC observed in *egl* null mutants. Instead, αC(3)G staining remains diffuse in all 16-cystocytes with one or two bright clumps of staining (Fig. 4C). This pattern suggests that either the nuclei are arrested prior to pachytene, before the completion of the mature SC, or alternatively *mio, egl* mutants form a defective SC. The ability of mutations in *mio* to enhance the severity of the egl^{null} SC phenotype confirms that *mio* functions prior to the pachytene stage of meiosis.

The molecular characterization of the *mio* gene

Recombination mapping placed the *mio* gene on the left arm of the second chromosome between 4.52 cM and 5.10 cM. Using genomic deficiencies we mapped the *mio* gene to a small cytogenetic interval, 22D5-E1, consistent with the meiotic map position (Fig. 5A). Specifically, the *mio* ovarian phenotype is complemented by $Df(2L)dp^{79b}$ (22A2-3;22D5-E1) but not by $Df(2L)yan^{J2}$ [22C2;22E1 from Lai et al. (Lai et al., 1997)]. We molecularly defined the

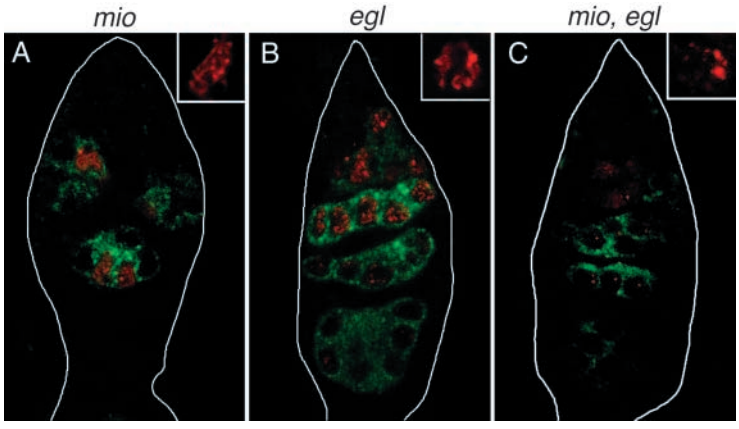

Fig. 4. *egl, mio* double mutants arrest prior to pachytene. *mio* is required at an early stage of meiosis. (A-C) Germaria double labeled with αC(3)G (red) and αOrb (green). Magnified C(3)G staining is shown in upper right panel. (A) *mio* mutant: two pro-oocytes have thick thread-like C(3)G pattern, indicating that, like wild type, the *mio* pro-oocytes progress to pachytene. (B) *egl* null mutant (egl^1): all 16 cells form the less extended SC that is representative of late zygotene or early pachytene. (C) mio^2, egl^1 double mutants: all 16 cells show the dot pattern of C(3)G that is normally observed in early zygotene.

proximal break points of *Df(2L)dp^{79b}* and *Df(2L)yan^{J2}* as 22C3 and 22D2, respectively, by quantitative Southern blot analysis (data not shown). This placed the *mio* gene within a 50 kb genomic region that contained 11 ORFs as predicted by BDGP (Fig. 5A). The 11 ORFs were sequenced from both the *mio^{1}* and *mio^{2}* chromosomes. *mio^{1}* and *mio^{2}* both contain a single nucleotide change in the *CG7074* ORF (nomenclature is taken from BDGP) that result in a nonsense mutation (Fig. 5A,C). No sequence alterations were found in the other 10 ORFs. *CG7074* encodes a single transcript of ~3 kb as determined by northern blot analysis (Fig. 5B), and a protein of 867 amino acids. Both *mio^{1}* and *mio^{2}* mutants are predicted to produce truncated proteins that contain 110 amino acids and 817 amino acids, respectively (Fig. 5C). To confirm that *CG7074* corresponds to the *mio* gene, we rescued the *mio* mutant phenotype using germline specific expression of full-length *CG7074* cDNA. As indicated in Table 2, UASp-CG7074 expressed by the germline specific nanos-Gal4:VP16 driver fully rescued the *mio^{2}* phenotype. Ovaries from rescued females did not contain polyploidy oocytes. In addition, although oogenesis in *mio^{2}* homozygotes is blocked at approximately stage 5, rescued *mio^{2}* ovaries exhibit no developmental block and are fully fertile (data not shown). These data formally demonstrate that *CG7074* is *mio* and indicate that the *mio* phenotype is germline dependent.

The *mio* gene is predicted to encode a novel protein that is highly conserved from yeast to mammals with the most closely related gene, human FLJ20323, sharing 30% identity and 47% similarity with *Drosophila mio* (from BLAST2 analysis, NCBI). The conservation between *mio* homologs is found throughout the length of the protein. However, the Mio protein does contain two highly conserved domains that are particular noteworthy (Fig. 5C). The first domain consists of four WD40 repeats near the N terminus of the protein. WD40 repeats can function as an interface for protein-protein interactions (Smith et al., 1999). The second domain, near the C terminus of the Mio protein, consists of ten invariant cysteines as well as three invariant histidines and contains limited structural similarity to the RING finger and PHD finger domains (Capili et al., 2001) (Fig. 5C).

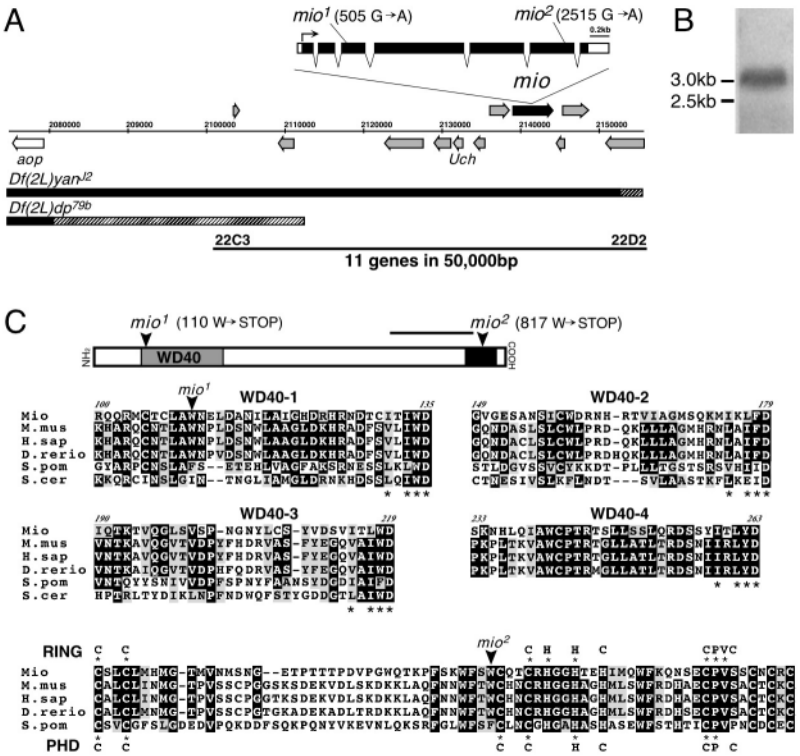

Fig. 5. Identification of the *mio* gene (A) The physical map of the 23C-D cytogenetic interval. Black boxes indicate the regions that are deleted in each deficiency. Light hatched boxes are the regions of uncertainty. The *mio* (*CG7074*) ORF is shown as black box with arrow indicating the direction of transcription. The other 10 ORFs in the defined 50 kb interval are depicted as grey arrows. The *mio* gene is composed of seven exons. (B) The *mio* gene encodes a single transcript. Northern blot of total RNA from wild-type ovaries, probed with a *mio* cDNA. (C) The Mio protein contains an N-terminal domain with four WD40 repeats (grey box) and a RING/PHD finger-like domain near the C terminus (black box). An alignment of the four WD40 repeats and the RING/PHD finger-like domain of Mio, human FLJ20323, mouse BC20002, zebrafish BC047198, fission yeast SPAC630.02 and budding yeast YBL104c. The locations of the mio^{1} and *mio^{2}* truncations are indicated (arrowhead). Both yeast homologs lack the last WD40 repeat, while the mammalian homologs contain six WD40 repeats, two more than are found in *Drosophila*. All homologs except YBL104c contain a RING/PHD finger-like domain. (YBL104c shares only part of the conserved domain.) Black bar above the structure shows the region used as antigen. Stars indicate amino acid conservation between *mio* homologs and the indicated motifs. The consensus for the RING finger and PHD finger motifs are shown, respectively, above and below the *mio* alignments.

Mio localizes to nuclei that contain synaptonemal complexes

In order to determine the precise cellular localization of the Mio protein, we generated antibodies against a C-terminal region of the protein (Fig. 5C). Western blot analysis indicates that the polyclonal antibody recognizes a single band of ~98.6 kDa, the predicted molecular weight of the Mio protein (Fig. 6A). The intensity of the 98.6 kDa band is dramatically increased in ovarian extracts from *UASp-mio; nanos-Gal4:VP16* females, which overexpress the *mio* mRNA (Fig. 6A). Ovaries from *mio^{2}* females produce a slightly smaller protein, 92.6 kDa, consistent with the *mio^{2}* C-terminal truncation. Immunostaining of wild-type ovaries indicates that the Mio protein specifically localizes to oocyte nuclei (Fig. 6B). Weak Mio staining is first detected in one or two centrally located cystocytes in region 2a (Fig. 6C). The staining becomes dramatically brighter and restricted to a single cell in region 2b. Staining in the oocyte nucleus after stage 3 is still visible

Table 2. Rescue of *mio* mutant phenotype by *mio* cDNA

Maternal genotype	*n*	16-nurse cell (%)	Wild type (%)
w; mio^{2}, UASp-mio	110	89.1	10.9
w; mio^{2}, UASp-mio; nos-GAL4/+	176	0.6	99.4

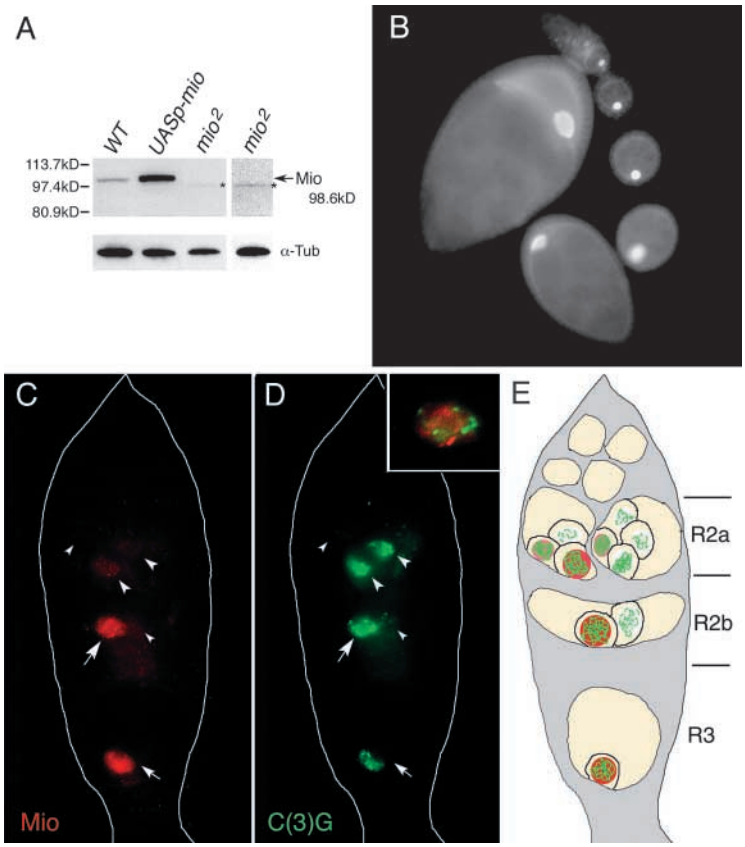

Fig. 6. Mio localizes to oocyte nuclei. (A) Western blot analysis of ovarian protein extracts. The αMio antibody recognizes a single band that coincides with the predicted molecular size of Mio, 98.6 kDa in extract from wild type (WT) and the Mio overexpression line (UASp-mio). Additionally, the antibody recognizes a slightly smaller protein (asterisk) in *mio*^{2} ovarian extracts. *mio*^{2} is predicted to encode a truncated Mio protein of 92.6 kDa. The last lane is a higher contrast picture of the *mio*^{2} extract. (B) A wild-type ovariole stained with αMio. (C) Faint Mio signal is detected in two cells of a cyst in region 2a. The pattern is often not symmetric, with one nucleus (large arrow) frequently having a brighter signal. In region 2b and region 3, the staining is restricted to a single cell and dramatically increases in intensity (arrows). (D) C(3)G localization in the same germarium as depicted in C. Small box denotes magnified region-2b nucleus stained with αMio (red) and αC(3)G (green). Arrows and arrowheads indicate αMio-positive cells in B and αC(3)G-positive cells in D. E is a diagram showing the stages and localization of Mio (red) and C(3)G (green) in the germarium depicted in C and D. The Mio protein colocalizes to the nuclei that stain most intensely with αC(3)G in region 2a (large arrowheads and arrows). However, the overlay of a region 2b nucleus demonstrates that the Mio protein has a different distribution than the SC component C(3)G (small box).

in some *mio*^{1} mutant egg chambers, indicating that the αMio signal observed in post-germarial stages of oogenesis is at least partially due to a crossreaction. However, we believe that the following two observations indicate that the αMio signal in the germarium is real. First, no germarial staining is observed in the *mio*^{1} mutant (see Fig. S1A at http://dev.biologists.org/supplemental), which is predicted to produce a truncated protein that does not contain the appropriate antigen (see Fig. 5C). Second, the αMio signal is dramatically increased in intensity, but present in the same germarial pattern, when the gene is overexpressed in the germline from a *mio* transgene (see Fig. S1B,C at http://dev.biologists.org/supplemental).

The Mio staining pattern is similar to proteins that localize to the pro-oocytes. Double labeling with αMio antibodies and an antibody against the SC protein C(3)G, indicate that Mio colocalizes to nuclei that contain the SC (Fig. 6D). However, Mio does not specifically localize to the thread-like SC itself, but appears to have a more dispersed distribution within the pro-oocyte nuclei (Fig. 6D, small box). Thus, the Mio protein accumulates in the nuclei of the pro-oocyte(s) at, or soon after, the onset of prophase of meiosis I. Double labeling with αMio and antibodies against the cytoplasmic oocyte determinant Orb, confirm that Mio is concentrated in the pro-oocyte nuclei beginning in region 2a (data not shown). This makes Mio one of the earliest nuclear markers for the oocyte that is not a known component of the synaptonemal complex.

The *mio* phenotype is suppressed by blocking the formation of DSB during meiosis

Mutations in genes required to repair DSB, such as *okr* and *spnB*, affect the formation of the dorsoventral axis of the egg (Ghabrial et al., 1998). In *okra* and *spnB* mutants this phenotype is suppressed by blocking the formation of the DSB that initiate meiotic recombination (Ghabrial and Schüpbach, 1999). In order to determine if blocking the formation of DSBs suppresses the *mio* ovarian phenotypes, we examined *mio*, *mei-W68* and *mio*, *mei-P22* double-mutant females. Both *mei-W68* (*SPO11* homolog) and *mei-P22* (novel gene) are required for DSB formation during meiosis (McKim and Hayashi-Hagihara, 1998; Sekelsky et al., 1999; Liu et al., 2002). Intriguingly, ovaries from *mio, mei-W68* and *mio, mei-P22* double-mutants have three to four times more egg chambers that contain an oocyte than *mio* single mutants (Table 3). In addition, *mio, mei-W68* and *mio, mei-P22* egg chambers often undergo vitellogenesis and develop to late stages of oogenesis (Fig. 7B). By contrast, egg chambers from *mio* single mutants rarely develop beyond stage 5 (Fig. 7A). Placing a single copy of either a *mei-W68* or *mei-P22* mutation in the *mio* background results in a partial suppression of the ovarian phenotype (Table 3). Thus, inhibiting the formation of DSBs during meiosis significantly suppresses the *mio* 16-nurse cell phenotype and the associated developmental delay.

The *spnB* and *okr* DV patterning defects are suppressed in a *mei-41* background (Ghabrial and Schüpbach, 1999). *mei-41* encodes the ATM/ATR homolog and is proposed to be a component of the pathway that delays meiotic progression in response to unrepaired DSB (Ghabrial and Schüpbach, 1999; McKim et al., 2000). These data indicate that it is the activation of the meiotic checkpoint, and not the presence of DSB, that cause the DV patterning defects observed in *okr* and *spnB* egg chambers. We examined *mei-41*^{29D}, *mio*^{2} double mutants to determine if the *mio* phenotype was also dependent on the activation of the meiotic checkpoint. In contrast to what is observed in *spn-B* and *okr* mutants, *mio*^{2} is not rescued in a *mei-41*^{null} background (Table

Table 3. Suppression of *mio* mutant phenotype by *mei-W68 and mei-P22* mutations

Maternal genotype	*n*	16-nurse cell (%)	Abnormal karyosome (%)	Other* (%)	Wild type (%)
mio^2	411	89.5	2.0	1.7	6.8
mio^2, $mei\text{-}W68^1$/+	259	40.7	–	1.9	57.4
mio^1/mio^2, $mei\text{-}W68^1$/+	366	58.2	–	0.9	40.9
mio^2, $mei\text{-}W68^1$	368	21.6	18.4	2.9	57.1
mio^2; $mei\text{-}P22^{p22}$/+	444	56.4	8.4	8.4	29.7
mio^2; $mei\text{-}P22^{p22}$	153	13.6	7.5	5.6	73.3
mio^1/mio^2, $mei\text{-}W68^{k05603}$/+**	221	57.1	–	2.9	40.0
mio^2, $mei\text{-}W68^{k05603}$/+	562	60.0	–	5.3	34.7
mio^2 ***	224	99.1	0	0.9	0
$mei\text{-}41^{29D}$/+; mio^2 ***	342	98.8	0	0	1.2
$mei\text{-}41^{29D}$; mio^2 ***	202	99.0	0	0	1.0

*Egg chambers that have more than 16 cells in double mutants, and/or that have eight cells in mio^2.
**$mei\text{-}W68^{k05603}$ is homozygous lethal.
***mio^2 line used for the *mei-41* study was independently isolated from the $stil^3$ chromosome by meiotic recombination, and has a slightly stronger phenotype than the original mio^2 isolate.

3). These data indicate that the presence of unrepaired DSBs contribute to the *mio* phenotype independent of the meiotic checkpoint.

Discussion

mio encodes a highly conserved protein that localizes to oocyte nuclei in early prophase of meiosis I

The *mio* gene encodes a novel protein that is conserved from yeast to humans. In higher eukaryotes, all Mio family members share a similar domain structure. The N termini contain a series of four to six well-conserved WD40 repeats. WD40 repeats often provide a surface for protein-protein interactions (Smith et al., 1999). The WD40 repeats found in *mio* family members are most similar to those present in the chromatin-binding protein CAF1p48/RbAp48, which is a component of numerous chromatin-remodeling complexes (Vermaak et al., 1999; Mello and Almouzni, 2001). Specifically, CAF1p48/RbAp48 is found in complexes that modify chromatin through the acetylation and deacetylation of histones. The similarity between the WD40 repeats found in Mio and CAF1p48/RbAp48 is particularly intriguing in light of the disruptions in meiotic chromatin structure observed in *mio* single mutants as well as *mio, egl* double mutant combinations. In addition to the WD40 repeats, Mio family members contain a highly conserved 50 amino acid domain near their C termini that share structural similarities to two well-characterized zinc binding domains, the RING finger and the PHD finger. RING finger domains are present in a subclass of E3 ubiquitin ligases, while PHD fingers have been implicated in chromatin binding (Aasland et al., 1995; Joazeiro and Weissman, 2000). Although the 'Mio domain' does share structural similarities to these zinc-binding domains, it does not fit the exact consensus of either a canonical RING finger or a canonical PHD finger. Therefore, the biochemical function of this highly conserved domain remains to be empirically determined.

Mio is the earliest nuclear marker for the oocyte that is not a known component of the SC. In *Drosophila,* the SC is constructed before the formation of the DSBs that initiates meiotic recombination (McKim et al., 1998; Liu et al., 2002). The Mio protein is first expressed in region 2a where it colocalizes to nuclei that contain SCs. Thus, during oogenesis Mio is expressed specifically in cells that have entered the meiotic cycle. Although Mio is expressed in both pro-oocytes in early region 2a, Mio staining always appears asymmetric with one cell, presumably the true oocyte, having a brighter signal. Intriguingly, Mio staining is asymmetric before there is noticeable asymmetry in SC structure, as determined by C(3)G staining. Although Mio

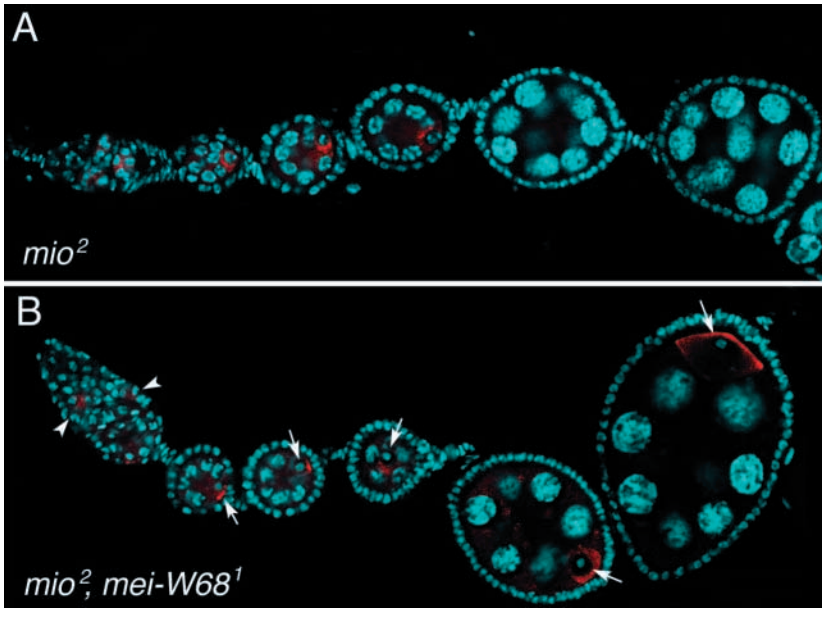

Fig. 7. Mutations in *mei-W68* suppress the *mio* mutant phenotype. Ovarioles from mio^2 (A) and a mio^2, $mei\text{-}W68^1$ double mutant (B), stained with Hoechst (blue) and αOrb (red). Unlike the single mutant, oocytes from double mutants form normal karyosomes (arrows) and accumulate Orb protein beginning in region 2a (arrowheads). Although most mio^2, $mei\text{-}W68^1$ egg chambers develop normally, some abnormalities are observed, such as the mispositioning of the oocyte (see third egg chamber in B where the oocyte is located in the center, rather than the posterior, of the egg chamber).

does accumulate soon after the onset of the meiotic cycle, in *egl* mutants, Mio does not localize to a single nucleus but remains undetectable. These data strongly suggest that the construction of the microtubule-based directional transport system precedes the specific accumulation of Mio in the oocyte. This localization pattern is consistent with a role for *mio* downstream of the initial specification of the oocyte identity.

Mio influences cyst polarity and oocyte differentiation

In *mio* mutant egg chambers, the oocyte enters the endocycle and adopts a nurse cell fate. Two observations indicate that Mio acts as early as region 2a and affects some of the earliest steps in oocyte differentiation. In wild-type cysts four cells enter meiosis and form SC in region 2a before the meiotic cycle is restricted to a single cell in region 2b. However, in *mio* mutants, too many cells enter meiosis in region 2a and form SC. This early broadening of the meiotic gradient, with too many cells displaying oocyte like features, is similar to what is observed in *par1* mutants and is consistent with a delay in the establishment of cyst polarity and/or the differentiation of the oocyte. In addition, *mio* mutants are slow to accumulate oocyte specific markers. In wild-type cysts, oocyte-specific markers, such as Orb and Bic-D, accumulate in a single centrally localized cell beginning in region 2a (Spradling, 1993). In *mio* mutants this accumulation is often not observed until region 3. Indeed, the initial expression of Orb appears to be delayed or substantially reduced, with *mio* cysts throughout the germarium having lower overall levels of Orb compared with similarly staged wild-type cysts. These data demonstrate that consistent with its expression at the onset of prophase of meiosis I, Mio functions early in oogenesis to promote the polarization of the cyst and acquisition of the oocyte fate. However, we note that it is not clear if this early meiotic function of Mio is required for the maintenance of the meiotic cycle or if Mio functions at multiple times during oogenesis.

How does one reconcile the limited expression pattern of Mio, which specifically accumulates in the nuclei of the two pro-oocytes, with the apparent global disruption in cyst polarity observed in *mio* mutants? We can think of at least two possible explanations for this apparent paradox. First, Mio may act in the oocyte nucleus to reinforce and maintain the oocyte fate. In this model, subtle alterations in oocyte differentiation may compromise, but not eliminate, the directional transport system and/or other pathways that are required to establish and/or reinforce cyst polarity. This might produce a weak *egl*-like phenotype and thus allow an inappropriate number of cells to enter meiosis. Alternatively, Mio may be present at undetectable levels in cells beyond the two pro-oocytes. In this model, Mio acts cell autonomously to influence cell cycle regulation and the establishment of cyst polarity in cells throughout the cyst.

Mio facilitates meiotic progression

The analysis of *mio, egl* double mutants demonstrate that Mio influences meiotic progression and/or meiotic chromosome structure early in prophase of meiosis I, prior to the formation of the mature SC. The phenotype of *mio, egl* double mutants is considerable stronger than either single mutant. In the double mutant the C(3)G pattern never appears even remotely thread-like, but persists as generalized nuclear staining with one or more bright dots. This pattern suggests that either the nuclei are arrested prior to pachytene, before the completion of the mature SC, or alternatively *mio, egl* mutants form a defective SC.

Why might the disruption of directional transport to the oocyte uncover an earlier function for *mio*? In wild-type cysts, factors required for meiotic progression are produced in all 16 cystocytes but are quickly transported to the oocyte where they accumulate to high levels (Spradling, 1993). In *egl* mutants these putative meiotic factors are not enriched in a single cell, but instead are present in all 16 cystocytes, presumably at a much lower concentration than is observed in a wild-type oocyte. It is only in this compromised situation, where factors required for meiotic progression may be limiting, that Mio becomes an absolute requirement for progression to pachytene. One possible explanation for these data is that a protein that is normally concentrated in the oocyte, via the direction transport system, is partially redundant for Mio function. Additional support for a role for Mio prior to pachytene comes from the observation that *mio* single mutants contain an increased proportion of cysts with fragmented or partially formed SC in region 2a of the germarium. The increase in the proportion of this developmental intermediate suggests that mutations in *mio* cause subtle alterations in the kinetics of SC formation.

Our data support a model in which Mio acts to facilitate the nuclear events of meiotic progression soon after the completion of premeiotic S phase and the onset of the meiotic developmental program. Considering the presence of WD40 repeats similar to those found in CAF1p48/RbAp48, we speculate that Mio may act to modify chromatin structure in the pro-oocyte nuclei to promote oocyte differentiation and prepare the oocyte nucleus for the upcoming events of meiosis, including meiotic recombination and the meiotic divisions. As discussed below, this model is consistent with a potential role for Mio in DSB repair during meiosis.

Mio may be required to repair the DSBs that initiate meiotic recombination

The *mio* ovarian phenotype is suppressed by inhibiting the formation of DSBs during meiosis. In *mio* single mutants, the oocyte frequently enters the endocycle and becomes polyploid. However, when placed in a genetic background in which DSB formation is inhibited, the majority of *mio* egg chambers retain an oocyte and develop to late stages of oogenesis. Intriguingly, mutations in the meiotic checkpoint gene *mei-41* do not suppress *mio*, indicating that it is the physical presence of DSB, and not the activation of the meiotic checkpoint, that contributes to the *mio* phenotype. However, although clearly important, the inability to repair DSBs during meiosis is unlikely to be sole cause of the *mio* phenotype. Mutations in genes with a direct role in DSB repair, such as *okr* and *spnB*, cause patterning defects late in oogenesis (Gonzalez-Reyes et al., 1997; Ghabrial et al., 1998) but do not result in the complete abandonment of meiosis and the polyploidization of the oocyte, as is observed in *mio* mutants. Therefore, *mio* must have additional functions beyond the repair of DSBs. Considering that Mio localizes to the oocyte nucleus early in meiosis and functions before the construction of the mature SC, we speculate that *mio* acts upstream of the enzymology of DSB repair. Thus, the inability of *mio* mutants to repair DSB

may be due to a general alteration in meiotic chromosome structure or alternatively subtle alterations in the meiotic program.

In the future, the identification of the molecular mechanism by which *mio* influences the differentiation of the oocyte nucleus as well as the regulation of the meiotic chromosomes will provide insight into the poorly understood pathways that drive early meiotic progression and early oocyte development in metazoans.

We thank Trudi Schüpbach, Zhi-Chun Lai, Tin Tin Su and the Bloomington stock center for fly stocks; the Developmental Studies Hybridoma Bank and Ruth Steward for antibodies; Kim McKim for helpful discussions on SC formation; and Robert DeLotto and members of the Lilly laboratory for critically reading of the manuscript. We thank George Patterson for help with confocal microscopy. T.I. is a Japan Society for the Promotion of Science Research Fellow in Biomedical and Behavioral Research at the NIH.

References

Aasland, R., Gibson, T. J. and Stewart, A. F. (1995). The PHD finger: implications for chromatin-mediated transcriptional regulation. *Trends Biochem. Sci.* **20**, 56-59.

Capili, A. D., Schultz, D. C., Rauscher, F. J. and Borden, K. L. B. (2001). Solution structure of the PHD domain from the KAP-1 corepressor: structural determinants for PHD, RING and LIM zinc-binding domains. *EMBO J.* **20**, 165-177.

Carpenter, A. T. C. (1994). *egalitarian* and the choice of cell fates in *Drosophila* melanogaster oogenesis. In *Ciba Foundation Symposium 182, Germline Development* (ed. J. Marsh and J. Goode), pp. 223-245. London: John Wiley.

Christerson, L. B. and McKearin, D. (1994). orb is required for anteroposterior and dorsoventral patterning during Drosophila oogenesis. *Genes Dev.* **8**, 614-628.

Clark, K. A. and McKearin, D. M. (1996). The Drosophila stonewall gene encodes a putative transcription factor essential for germ cell development. *Development* **122**, 937-950.

Cooley, L. and Theurkauf, W. E. (1994). Cytoskeletal functions during *Drosophila* oogenesis. *Science* **266**, 590-596.

de Nooij, J. C., Graber, K. H. and Hariharan, I. K. (2000). Expression of the cyclin-dependent kinase inhibitor Dacapo is regulated by Cyclin E. *Mech. Dev.* **97**, 73-83.

Ghabrial, A., Ray, R. P. and Schüpbach, T. (1998). *okra* and *spindle-B* encode components of the RAD52 DNA repair pathways and affect meiosis and patterning in Drosophila oogenesis. *Genes Dev.* **12**, 2711-2723.

Ghabrial, A. and Schüpbach, T. (1999). Activation of a meiotic checkpoint regulates translation of Gurken during *Drosophila* oogenesis. *Nat. Cell Biol.* **1**, 354-357.

Gonzalez-Reyes, A., Elliott, H. and St Johnston, D. (1997). Oocyte determination and the origin of polarity in *Drosophila*: the role of the spindle genes. *Development* **124**, 4927-4937.

Grieder, N. C., de Cuevas, M. and Spradling, A. C. (2000). The fusome organizes the microtubule network during oocyte differentiation in *Drosophila*. *Development* **127**, 4253-4264.

Hong, A., Lee-Kong, S., Iida, T., Sugimura, I. and Lilly, M. A. (2003). The p27cip/kip ortholog dacapo maintains the Drosophila oocyte in prophase of meiosis I. *Development* **130**, 1235-1242.

Huynh, J. R., Shulman, J. M., Benton, R. and St Johnston, D. (2001). PAR-1 is required for the maintenance of oocyte fate in Drosophila. *Development* **128**, 1201-1209.

Huynh, J. R. and St Johnston, D. (2000). The role of BicD, Egl, Orb and the microtubules in the restriction of meiosis to the *Drosophila* oocyte. *Development* **127**, 2785-2794.

Joazeiro, C. A. P. and Weissman, A. M. (2000). RING finger protein: mediators of ubiquitin ligase activity. *Cell* **102**, 549-552.

Koch, E. A. and Spitzer, R. H. (1985). Multiple effects of colchicine on oogenesis in Drosophila: induced sterility and switch of potential oocyte to nurse-cell developmental pathway. *Cell Tissue Res.* **228**, 21-32.

Lai, Z. C., Fetchko, M. and Li, Y. (1997). Repression of *Drosophila* photoreceptor cell fate through cooperative action of two transcriptional repressors Yan and Tramtrack. *Genetics* **147**, 1131-1137.

Lantz, V., Ambrosio, L. and Schedl, P. (1992). The *Drosophila orb* gene is predicted to encode sex-specific germline RNA-binding proteins and has localized transcripts in ovaries and early embryos. *Development* **115**, 75-88.

Lantz, V., Chang, J. S., Horabin, J. I., Bopp, D. and Schedl, P. (1994). The Drosophila orb RNA-binding protein is required for the formation of the egg chamber and establishment of polarity. *Genes Dev.* **8**, 598-613.

Laurençon, A., Purdyb, A., Sekelsky, J., Hawley, R. S. and Su, T. T. (2003). Phenotypic Analysis of Separation-of-Function Alleles of MEI-41, Drosophila ATM/ATR. *Genetics* **164**, 589-601.

Liu, H., Jang, J. K., Kato, N. and McKim, K. S. (2002). mei-P22 encodes a chromosome-associated protein required for the initiation of meiotic recombination in Drosophila melanogaster. *Genetics* **162**, 245-258.

Liu, Z., Xie, T. and Steward, R. (1999). Lis1, the Drosophila homolog of a human lissencephaly disease gene, is required for germline cell division and oocyte differentiation. *Development* **126**, 4477-4488.

Mach, J. M. and Lehmann, R. (1997). An Egalitarian-BicaudalD complex is essential for oocyte specification and axis determination in Drosophila. *Genes Dev.* **11**, 423-435.

Mahowald, A. P. and Kambysellis, M. P. (1980). Oogenesis. In *Genetics and Biology of* Drosophila (ed. M. Ashburner and T. R. F. Wright), pp. 141-224. London: Academic Press.

McKim, K. S., Green-Marroquin, B. L., Sekelsky, J. J., Chin, G., Steinberg, C., Khodosh, R. and Hawley, R. S. (1998). Meiotic synapsis in the absence of recombination. *Science* **279**, 876-878.

McKim, K. S. and Hayashi-Hagihara, A. (1998). mei-W68 in Drosophila melanogaster encodes a Spo11 homolog: evidence that the mechanism for initiating meiotic recombination is conserved. *Genes Dev.* **12**, 2932-2942.

McKim, K. S., Jang, J. K., Sekelsky, J. J., Laurençon, A. and Hawley, R. S. (2000). mei-41 is required for precocious anaphase in Drosophila females. *Chromosoma* **109**, 44-49.

Mello, J. A. and Almouzni, G. (2001). The ins and outs of nucleosome assembly. *Curr. Opin. Genet. Dev.* **11**, 136-141.

Mulligan, P. K., Campos, A. R. and Jacobs, J. R. (1996). Mutations in the gene stand still disrupt germ cell differentiation in Drosophila ovaries. *Dev. Genet.* **18**, 316-326.

Page, S. L. and Hawley, R. S. (2001). *c(3)G* encodes a *Drosophila* synaptonemal complex protein. *Genes Dev.* **15**, 3130-3143.

Pare, C. and Suter, B. (2000). Subcellular localization of Bic-D::GFP is linked to an asymmetric oocyte nucleus. *Development* **113**, 2119-2127.

Ran, B., Bopp, R. and Suter, B. (1994). Null alleles reveal novel requirements for Bic-D during Drosophila oogenesis and zygotic development. *Development* **120**, 1233-1242.

Robinson, D. N. and Cooley, L. (1996). Stable intercellular bridges in development: the cytoskeleton lining the tunnel. *Trends Cell Biol.* **6**, 474-479.

Rørth, P. (1998). Gal4 in the *Drosophila* female germline. *Mech. Dev.* **78**, 113-118.

Schüpbach, T. and Wieschaus, E. (1991). Female sterile mutations on the second chromosome of *Drosophila melanogaster*. II. Mutations blocking oogenesis or altering egg morphology. *Genetics* **129**, 1119-1136.

Sekelsky, J. J., McKim, K. S., Messina, L., French, R. L., Hurley, W. D., Arbel, T., Chin, G. M., Deneen, B., Force, S. J., Hari, K. L. et al. (1999). Identification of novel Drosophila meiotic genes recovered in a P-element screen. *Genetics* **152**, 529-542.

Smith, T. F., Gaitatzes, C., Saxena, K. and Neer, E. J. (1999). The WD repeat: a common architecture for diverse functions. *Trends Biochem. Sci.* **24**, 181-185.

Spradling, A. C. (1986). P element-mediated transformation. In Drosophila*: A Practical Approach* (ed. D. B. Roberts), pp. 175-197. Oxford: IRL Press.

Spradling, A. C. (1993). Developmental genetics of oogenesis. In *The Development of* Drosophila melanogaster, Vol. I (ed. M. Bate and A. Martinez Arias), pp. 1-70. New York: Cold Spring Harbor Laboratory Press.

Suter, B. and Steward, R. (1991). Requirement for phosphorylation and localization of the Bicaudal-D protein in Drosophila oocyte differentiation. *Cell* **67**, 917-926.

Swan, A., Nguyen, T. and Suter, B. (1999). Drosophila Lissencephaly-1 functions with Bic-D and dynein in oocyte determination and nuclear positioning. *Nat. Cell Biol.* **1**, 444-449.

Theurkauf, W. E., Smiley, S., Wong, M. L. and Alberts, B. M. (1992). Reorganization of the cytoscheleton during *Drosophila* oogenesis: implications for axis specification and intercellular transport. *Development* **115**, 923-936.

Theurkauf, W. E., Alberts, B. M., Jan, Y. N. and Jongens, T. A. (1993). A central role for microtubules in the differentiation of *Drosophila* oocytes. *Development* **118**, 1169-1180.

Vaccari, T. and Ephrussi, A. (2002). The fusome and microtubules enrich Par-1 in the oocyte, where it effects polarization in conjunction with Par-3, BicD, Egl, and Dynein. *Curr. Biol.* **12**, 1524-1528.

Van Buskirk, C. and Schüpbach, T. (1999). Versatility in signalling: multiple responses to EGF receptor activation during *Drosophila* oogenesis. *Trends Cell Biol.* **9**, 1-4.

Van Doren, M., Williamson, L. A. and Lehmann, R. (1998). Regulation of zygotic gene expression in Drosophila primordial germ cells. *Curr. Biol.* **12**, 243-246.

Vermaak, D., Wade, P. A., Jones, P. L., Shi, Y. B. and Wolffe, A. P. (1999). Functional analysis of the SIN3-histone deacetylase RPD3-RbAp48-Histone H4 connection in the *Xenopus* oocyte. *Mol. Cell. Biol.* **19**, 5847-5860.

Wharton, R. P. and Struhl, G. (1989). Structure of the Drosophila *BicaudalD* protein and its role in localizing the posterior determinant *nanos*. *Cell* **59**, 881-892.